

LETTER TO THE EDITOR

Far-infrared excitations in antidot systems on silicon MOS structures

A Huber†, I Jejina†, H Lorenz†, J P Kotthaus†, S Bakker‡ and T M Klapwijk‡

† Sektion Physik der LMU München, D-80539 München, Germany

‡ University of Groningen, Department of Applied Physics, Nijenborgh 4, NL-9747 AG Groningen, The Netherlands

Received 1 December 1994, accepted for publication 19 January 1995

Abstract. We report on far-infrared transmission measurements of an antidot superlattice in a stacked-gate silicon MOS device. The electrons in this antidot system are electrostatically confined below the metallic mesh of the bottom gate. Sweeping the top gate voltage allows to tune the electron system from a two-dimensional electron system to an antidot superlattice. The observed magnetic field dispersion of the electronic oscillations is in good agreement with a recently developed classical theory.

As characteristic modes of low-dimensional systems, the collective electronic excitations in an antidot matrix have recently attracted much attention [1–7]. Such an antidot array consists of a two-dimensional electron system (2DES) with islands acting as repulsive areas for electrons. Up to now far-infrared (FIR) transmission experiments have predominantly been performed in InGaAs/AlInAs [1] and GaAs/AlGaAs [2, 3] heterostructures with a low effective electron mass of $m^* = 0.042m$ and $m^* = 0.067m$ respectively. The lower effective mass and the higher electron mobility favour these material systems compared to Si ($m^* = 0.2m$). Stimulated by the above-mentioned experiments, different theories have been proposed to explain the experimental results [4–7]. The collective excitation spectrum of antidots in a magnetic field B is dominated by two branches. The high-frequency mode (ω_1) possesses a finite energy at $B = 0$ T and approaches the cyclotron resonance energy at high magnetic fields. At low magnetic fields this mode exhibits a weak or slightly negative dispersion. The low-frequency mode (ω_2) first follows the cyclotron frequency and then shows a negative dispersion with increasing magnetic field. At high magnetic fields and in a classical one-particle picture the ω_1 mode (ω_2 mode) represents an electron propagating in between (around) the antidots.

In the present work we investigate the collective excitations in an antidot superlattice on silicon. The antidot matrix is induced below the metallic lower gate in a stacked-gate silicon sample [8, 9]. Our analysis reveals that the cyclotron resonance (CR) is no fundamental excitation in an antidot system. The measured magnetic

field dispersion can be well understood by calculating the collective excitation spectra in an array of antidots in the effective medium approximation.

The stacked-gate devices are fabricated on a p-type (001) Si wafer with low boron substrate doping concentration ($N_{\text{boron}} \approx 1 \times 10^{14} \text{ cm}^{-3}$) and with a thermal oxide of thickness $d_1 = 101$ nm. A periodic metallic mesh serving as a bottom gate is defined using laser holography and a lift-off step. A PECVD (plasma enhanced chemical vapour deposition) oxide of thickness $d_2 = 125$ nm is sandwiched between the structured bottom and the homogeneous top gate. The geometrical width w of a single antidot is 370 nm, the period a is 740 nm.

The transmission T of the sample is measured in a FIR Fourier transform spectrometer at $T = 2$ K with a magnetic field perpendicular to the device surface. At very low temperatures above-bandgap light is needed to induce an electron inversion layer in these p-type MOS (metal oxide semiconductor) capacitor structures. An infrared light-emitting diode (IR-LED) illuminates the sample during the recording of the spectra, to establish quasi-equilibrium in the presence of a small leakage current across the thermal oxide between the bottom gate and the substrate contact. The resistance across this oxide is about 40 M Ω under illumination. As a consequence, at voltages above the threshold voltage for electrons the photogenerated holes compensate the negatively charged acceptors and a quasi-accumulation layer of electrons is formed at the Si surface.

In the present case of small signals ($\Delta T/T \ll 1$) the relative change in transmission can be approximated by

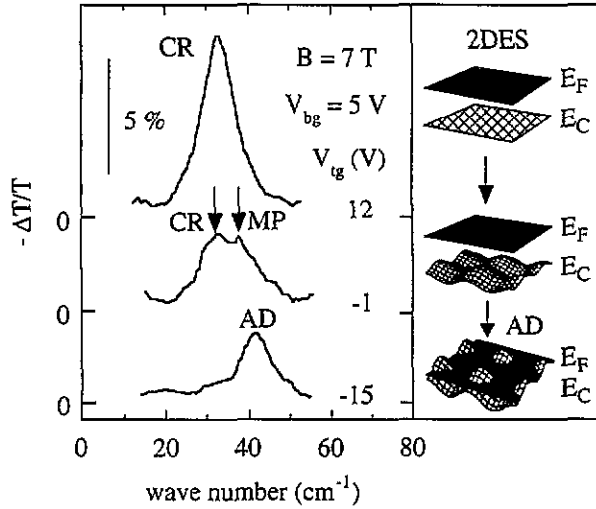


Figure 1. Transition from a 2DES (CR) via a modulated 2DES to an antidot superlattice (AD) by varying the top gate voltage (V_{tg}) for $B = 7$ T. Close to the threshold voltage for electrons below the top gate $V_{tg} = -1$ V, besides the CR a magnetoplasmon-like excitation (MP) is observed. The voltage at the bottom gate is fixed at 5 V. The sketch on the right illustrates the modulation of the subband edge E_C with respect to the Fermi energy E_F .

the following expression [10]:

$$-\frac{\Delta T}{T} = 1 - \frac{T(N_s)}{T(0)} \propto \text{Re}(\sigma(\omega)). \quad (1)$$

The last term of (1) represents the real part of the effective dynamic conductivity σ of the antidot system and N_s is the average two-dimensional carrier density.

We now introduce experimental results of collective excitations in antidot systems. The antidot system is defined electrostatically by applying appropriate gate voltages to the microstructured MOS sample, so that the transition from a quasi-two-dimensional electron system (both gates positively biased) to an antidot superlattice can be studied as exemplified in figure 1 for $B = 7$ T. It should be mentioned that in [9] the transition from a quasi-two-dimensional electron system to a dot superlattice is studied.

At fixed bottom gate voltage $V_{bg} = 5$ V the electron system can be tuned from a 2DES (top gate voltage $V_{tg} = 12$ V) to an antidot structure ($V_{tg} = -15$ V). In the aforementioned case a pronounced cyclotron resonance (CR) of a 2DES is observed. In the antidot configuration, the CR mode has disappeared and only the antidot signal remains. Only close to the threshold voltage for inversion electrons below the top gate at $V_{tg} = -1$ V do we observe besides the CR a magnetoplasmon-like resonance of a strongly density-modulated electron system [11]. Both resonances are indicated by arrows. By fitting the spectra for different V_{tg} with equation (2) (see below) using one Lorentz curve, we find a maximum of the linewidth of the resonance in the transition regime ($V_{tg} = -1$ V), a further hint that the spectrum consists of two resonances.

In figure 2 spectra are shown for different magnetic fields where an electron antidot mesh is formed below

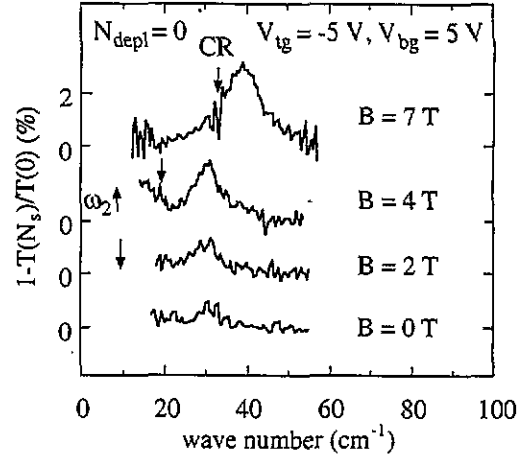


Figure 2. Antidot modes in a magnetic field. For $B = 4$ T the shoulder of the low energetic resonance ω_2 (theoretical value is indicated by an up arrow) at low wavenumbers is observed ($N_{depl} = 0$). The cyclotron resonance (CR) positions for $m^* = 0.2m$ are indicated by down arrows.

the bottom gate. For $B = 0$ T a resonance with little oscillator strength is observed. Until $B = 4$ T this resonance does not shift markedly in its energetic position but the absorption amplitude increases. For $B = 4$ T an additional absorption signal at low wavenumbers emerges, which is interpreted as the high-energy shoulder of the low-frequency mode (ω_2) in an antidot superlattice. The two main excitations in an antidot system exchange oscillator strength [6]. Therefore it is expected, as our experiment demonstrates, that we should observe the lower branch at medium magnetic fields. At even higher magnetic fields the dominant upper resonance shifts to higher energies and approaches the cyclotron resonance energy. To evaluate the resonance positions and the oscillator strength the antidot spectra were fitted within a classical harmonic oscillator model. Combined with formula (1) the result is

$$-\frac{\Delta T}{T} = \frac{2}{c\epsilon_0 (1 + \sigma_g/c\epsilon_0 + \sqrt{\epsilon_{Si}})} \frac{N_s e^2}{m^*} \times \frac{\omega^2/\tau}{\omega^2/\tau^2 + (\omega_i^2 - \omega^2)^2}. \quad (2)$$

$c\epsilon_0$ denotes the wave admittance of free space, σ_g the conductivity of the NiCr gate ($\approx (1 \text{ k}\Omega \text{ }\square^{-1})^{-1}$), m^* the effective electron mass, ϵ_{Si} the dielectric constant of Si and τ the scattering relaxation time. In our model, the resonance frequency ω_i is equal to the high-frequency mode ω_1 . The extracted oscillator strength is revealed in figure 3. Up to $B = 2.5$ T this value is almost constant, then it increases and saturates for $B \geq 8$ T. The increase is about a factor of 10. This behaviour is typical for an antidot superlattice and has been quantitatively verified by theory [6] for the experimental data on InGaAs/AlInAs [1] and GaAs/AlGaAs [2, 3] heterostructures.

The measured resonance positions of the ω_1 mode are indicated by full circles in figure 4. For moderate fields

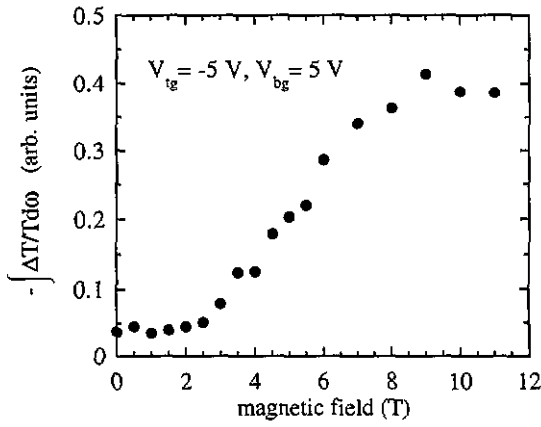


Figure 3. Oscillator strength for the high energetic antidot mode as a function of the magnetic field.

the dispersion is nearly constant with a slightly negative magnetic field dispersion. The qualitative development of the antidot branches can be explained in a simple model as repulsive interaction of two modes. Two modes are predestined for this interaction, which in the absence of interaction would become energetically degenerate in this low-dimensional system. One mode proposed is the cyclotron resonance and the other an edge mode around the antidot. Magnetoplasmons and dimensional resonances are inappropriate for such a repulsive interaction with the CR mode [12] because their energies always lie above the cyclotron energy. Both the CR and the edge mode, which is energetically degenerate with an edge mode in a quantum dot in the single-particle picture in high magnetic fields, are good descriptions of the excitations in a system with one antidot [7]. Furthermore, these two modes have the same polarization.

Using the effective medium approximation, the excitation spectrum of an array of antidots can be calculated [7]. This model uses classical electrodynamics and takes into account the interaction between antidots. The zeros of the equation

$$1 - \frac{1-f}{\Omega(\Omega \pm \Omega_c)} - \frac{f}{\Omega(\Omega \mp \Omega_c)} = 0 \quad (3)$$

give the resonance energies in an antidot system. Ω and Ω_c are dimensionless parameters with $\Omega = \omega/\omega_0$ and $\Omega_c = \omega_c/\omega_0$. The cyclotron frequency ω_c is determined by eB/m^* , ω_0 stands for the frequency of the high-frequency mode ω_1 at $B = 0$ T. The geometrical filling factor f is defined by $1 - A/a^2$. A is the area of a single antidot. The magnetic field dispersion consists of three branches: the branch with the highest energy plays a subordinate role due to its low oscillator strength. The high (ω_1) and the low energetic branch (ω_2) as the two dominant collective excitations are shown in figure 4 for different geometric filling factors. Here the experimental value $\omega_0 = 30.5$ cm⁻¹ is used for normalization. The curve for $f = 0.8$ best describes the experiment apart from some deviations at low magnetic fields. A dot area $A = \pi(a/4)^2$ describes the experimental geometry well and yields $f = 0.8$ in good agreement with the fit to

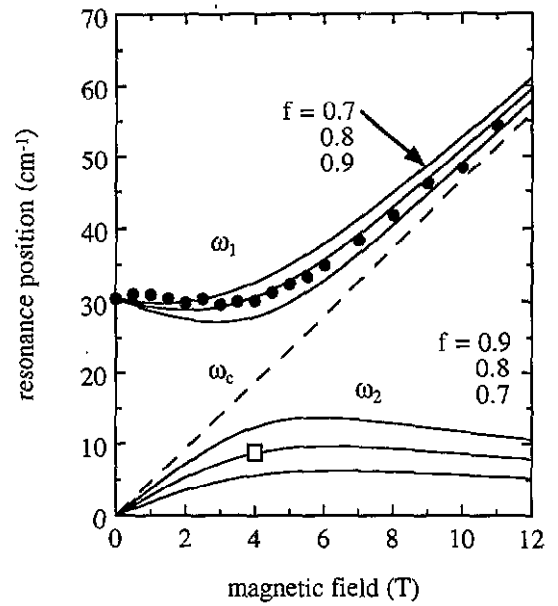


Figure 4. Measured magnetic field dispersion for the high energetic antidot mode (full circles). The curves correspond to the zeros of equation (3) determining the main branches ω_1 and ω_2 of an antidot system for different geometrical filling factors f . (The square symbol marks the resonance position of ω_2 for $f = 0.8$ and $B = 4$ T; see figure 2).

the mode dispersion. The ω_2 mode always lies below the spectral range of the spectrometer, whereby the oscillator strength decreases with increasing magnetic field [7]. Therefore only the high energetic shoulder of ω_2 , as indicated by an arrow in figure 3 at $B = 4$ T for $f = 0.8$, gives experimental evidence for the low energetic branch.

It should be mentioned that with an appropriate gate voltage configuration we are also able to realize quantum dots in our stacked-gate sample [8, 9]. For $V_g = 16$ V and $V_{bg} = -3$ V we measure the well known magnetic field dispersion of quantum dots with a parabolic potential shape [13]. Under these bias conditions the leakage current between the top gate and the substrate contact is negligible and as a consequence the IR-LED can be switched off after charging and the spectra recorded in the dark under inversion conditions.

We conclude our discussion as follows: a stacked-gate device realized on an Si MOS structure is used to study the collective excitations in an antidot superlattice. Appropriate gate voltages permit us to tune from a 2DES to an antidot matrix. We demonstrate that cyclotron resonance is not an eigenmode of the antidot superlattice. Also the absence of a prominent CR signal demonstrates the excellent homogeneity of our antidot samples. The main upper branch of the magnetic field dispersion is well explained in the effective medium approximation. So far the high effective mass of the electrons in Si prevents an unambiguous observation of the lower antidot branch. Nevertheless there are hints for this mode in a magnetic field regime, where it is expected.

We would like to thank A Lorke for valuable discussions and the Volkswagen foundation for financial support.

References

- [1] Kern K, Heitmann D, Grambow P, Zhang Y H and Ploog K 1991 *Phys. Rev. Lett.* **66** 1618
- [2] Lorke A, Kotthaus J P and Ploog K 1991 *Superlatt. Microstruct.* **9** 103
- [3] Zhao Y, Tsui D C, Santos M, Shayegan M, Ghanbari R A, Antoniadis D A and Smith H I 1992 *Appl. Phys. Lett.* **60** 1510
- [4] Lorke A 1992 *Surf. Sci.* **263** 307
- [5] Fessatidis A, Cui H L and Kühn O 1993 *Phys. Rev. B* **47** 6598
- [6] Wu Y and Zhao Y 1993 *Phys. Rev. Lett.* **71** 2114
- [7] Mikhailov S A and Volkov V A 1994 *Phys. Low-Dim. Struct.* **1** 31
- [8] Alsmeyer J, Batke E and Kotthaus J P 1990 *Phys. Rev. B* **41** 1699
- [9] Jejina I, Lorenz H, Kotthaus J P, Bakker S and Klapwijk T M 1993 *Solid State Commun.* **85** 601
- [10] Tsui D C, Allen S J Jr, Logan R A, Kamgar A and Coppersmith S N 1978 *Surf. Sci.* **73** 419
- [11] Lorke A, Kotthaus J P and Ploog K 1990 *Phys. Rev. Lett.* **64** 2559
- [12] Ando T, Fowler A B and Stern F 1982 *Rev. Mod. Phys.* **54** 437
- [13] Fock V 1928 *Z. Phys.* **47** 446